Impact of prompt-neutron corrections on final fission-fragment distributions

A. Al-Adili,[1,2] F.-J. Hambsch,[1] S. Pomp,[2] and S. Oberstedt[1]
[1]*European Commission, Joint Research Center (IRMM), B-2440 Geel, Belgium*
[2]*Division of Applied Nuclear Physics, Uppsala University, S-751 20 Uppsala, Sweden*
(Received 29 August 2012; published 5 November 2012)

Background: One important quantity in nuclear fission is the average number of prompt neutrons emitted from the fission fragments, the prompt neutron multiplicity, $\bar{\nu}$. The total number of prompt fission neutrons, $\bar{\nu}_{\rm tot}$, increases with increasing incident neutron energy. The prompt-neutron multiplicity is also a function of the fragment mass and the total kinetic energy of the fragmentation. Those data are only known in sufficient detail for a few thermal-neutron-induced fission reactions on, for example, ^{233,235}U and ^{239}Pu. The enthralling question has always been asked how the additional excitation energy is shared between the fission fragments. The answer to this question is important in the analysis of fission-fragment data taken with the double-energy technique. Although in the traditional approach the excess neutrons are distributed equally across the mass distribution, a few experiments showed that those neutrons are predominantly emitted by the heavy fragments.
Purpose: We investigated the consequences of the $\nu(A, \mathrm{TKE}, E_{\rm n})$ distribution on the fission fragment observables.
Methods: Experimental data obtained for the ^{234}U(n, f) reaction with a Twin Frisch Grid Ionization Chamber, were analyzed assuming two different methods for the neutron evaporation correction. The effect of the two different methods on the resulting fragment mass and energy distributions is studied.
Results: We found that the preneutron mass distributions obtained via the double-energy technique become slightly more symmetric, and that the impact is larger for postneutron fission-fragment distributions. In the most severe cases, a relative yield change up to 20–30% was observed.
Conclusions: We conclude that the choice of the prompt-neutron correction method has strong implications on the understanding and modeling of the fission process and encourages new experiments to measure fission fragments in coincidence with prompt fission neutrons. Even more, the correct determination of postneutron fragment yields has an impact on the reliable assessment of the nuclear waste inventory, as well as on the correct prediction of delayed neutron precursor yields.

DOI: 10.1103/PhysRevC.86.054601 PACS number(s): 24.75.+i, 25.85.Ec, 25.40.−h, 24.10.−i

I. INTRODUCTION

The main part of the energy released in binary low-energy fission is contained in the kinetic energy of the fission fragments. The rest is distributed among deformation and intrinsic excitation energy of the nascent fragments. As prompt fission neutrons are emitted essentially after scission has taken place, their number is a direct measure of the amount of energy stored in the fission fragments. Hence, the change in neutron multiplicity as a function of fragmentation, compound nuclear excitation, and kinetic energy of the fragments provides important insights into the energy partition at scission. In neutron-induced fission the kinetic energy of the incident neutron leads only to a weak dependence of the total kinetic energy (TKE) of the fission fragments, but leads to an increased excitation energy. The excess energy is mainly found in an enhanced average total number of neutrons, $\bar{\nu}_{\rm tot}$, and their kinetic energies [1]. The enhanced neutron emission with increasing incident neutron energy is well known and has been observed for many fissioning systems. However, less known is how the extra emitted neutrons are distributed among the two fission fragments. Classically it was assumed that all fragments equally share the extra excitation energy, leading to extra neutron emission averaged over all fission fragments. This assumption is nowadays still used in various works, where fission-fragment data as a function of incident neutron energy are measured with the double-energy method. The neutron multiplicity as a function of fragment mass and TKE, $\bar{\nu}(A, \mathrm{TKE})$, has been measured only for the major isotopes, as, for example, ^{235}U and ^{239}Pu, and mainly at thermal incident neutron energy. Scarce measurements took place at higher incident neutron energy, where in general only $\bar{\nu}_{\rm tot}(E_{\rm n})$ is known. The traditional method for correcting prompt neutron emission from fission-fragments, takes the $\bar{\nu}(A)$ measured at thermal neutron energy and scales the whole distribution with $\bar{\nu}_{\rm tot}$ measured at the particular incident neutron energy, $E_{\rm n} = 0$. However, in a few experiments a tendency has been observed that the excess of prompt neutrons emitted at higher incident neutron energies is mainly emitted from the heavy fragment, leaving the light fragment neutron multiplicity more or less constant [2,3]. Recently, theoretical models confirmed those experimental studies, disfavoring the method of an average increased neutron emission for both fragments [4–6].

In the present paper we investigate the effects of the two prompt-neutron emission correction methods on the fission-fragment mass and kinetic energy distributions. We determine the pre-neutron-emission mass and TKE distributions as well as the corresponding postneutron distributions obtained in the reaction ^{234}U(n, f) at two different incident neutron energies, 4 and 5 MeV, respectively. The following denotations will be further used to identify the two neutron-multiplicity distributions as introduced in the following discussion.

(i) Average method (AV). The increase in neutron multiplicity as a function of incident neutron energy, $E_{\rm n}$, is equally distributed amongst all fission fragments.

(ii) Heavy method (HE). Starting from mass $A = 120$, the increase in $\bar{\nu}_{\rm tot}$ is only distributed among the heavy fragments while $\bar{\nu}(A)$ remains fixed for the light fission fragments and as determined at thermal neutron energy.

The quantitative discussion of the two different neutron correction methods is given in the following.

II. BACKGROUND

The distribution of promptly emitted neutrons from fission fragments, $\bar{\nu}(A)$, shows a characteristic sawtooth shape as a function of fragment mass as demonstrated in Fig. 1(a). This dependence is explained as a result of the characteristic deformation energies stored in the nascent fragments at the scission point [1,9]. The dip around fragment mass $A \sim 130$ is the result of nearly spherical fragment shapes owing to doubly magic nuclear closed shell configurations ($N = 82$, $Z = 50$). Fragment masses around 105–115 for the light fragment and around 150–160 for the heavy fragment are much more deformed and, hence, show a high neutron multiplicity. This correlation between the number of emitted neutrons and the total excitation energy (TXE) in the fissioning system is well known. In addition, the average neutron emission number increases with incident neutron energy [see Fig. 1(b) for the reaction ^{234}U(n,f)]. The question about the share of TXE which each of the fragments receive has been subject of recent

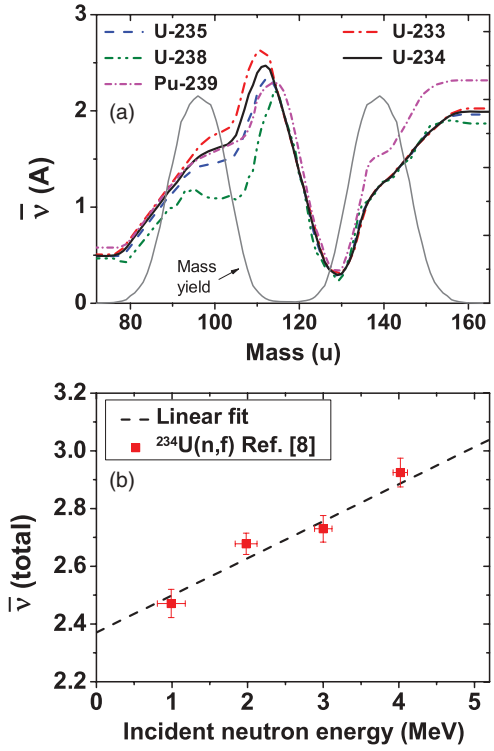

FIG. 1. (Color online) (a) Neutron-multiplicity distributions for the uranium isotopes together with the mass distribution for ^{234}U(n,f) (see text for details). The data for ^{233,235}U and ^{239}Pu are from Ref. [7]. (b) The total average neutron multiplicity $\bar{\nu}_{\rm tot}$ as a function of incident neutron energy. For ^{234}U a linear fit was used, based on Ref. [8].

theoretical investigations [4–6]. This has been performed in view of an improved modeling of the prompt neutron emission in fission to predict neutron emission multiplicities for isotopes for which this quantity has not been measured.

In most of the fission experiments, the neutron evaporation was not measured together with the fission fragments (see, e.g., Refs. [10,11]). To be able to calculate pre-neutron-emission fission-fragment properties, a parametrization for the prompt-neutron multiplicity as a function of fission-fragment mass was used to allow for an estimation of the number of emitted neutrons. The dependency on incident neutron energy was parametrized using either experimental data or evaluated files. In this type of correction, the average excess of neutron evaporation owing to increasing excitation energy is shared by both fragments, that is, AV correction method, which is demonstrated for instance in Refs. [10–13].

However, as mentioned above, experimental results from Refs. [2,3] showed that the extra neutron evaporation is mainly shared by the heavy fragments as the incident neutron energy increases. The measurements were performed at incident neutron energies 0.8 and 5.55 MeV and showed for ^{237}Np(n,f) and ^{235}U(n,f) an increase of the neutron multiplicity mainly for heavy fragments. The same dependence of $\bar{\nu}(A)$ was observed for proton-induced fission on ^{233,238}U [14–16], eventually putting doubt on the validity of the AV method.

Today, different theoretical models attempt to explain this particular behavior and are subject of a debate. One of which uses a thermodynamical explanation as the basis of this difference [4,5]. It has been shown that the nuclear temperature is constant up to excitation energies of 20 MeV. Based on the constant-temperature formula of Ref. [17], the energy-independent FF temperature is related to the fragment mass by $T \propto A^{-2/3}$. Thus, the light fragment is hotter than the heavy fragment, already before scission has occurred. Because both fragments are in contact before the scission point, the excess energy is transferred to the heavy fragment to reach equilibrium, similar to heat transfer processes. The result of this "energy sorting" is that the excess intrinsic excitation energy ends up in the heavy fragments which, as a consequence, emit more neutrons after scission [4,5]. The correct neutron emission procedure is still under debate. This work cannot prove the one or the other method right. However, we explore the consequences of the different neutron multiplicity correction methods on the final fragment distributions. For that, we profit from recently measured fission-fragment data from ^{234}U(n,f) [18]. Before we discuss the obtained distributions we will give a short introduction to the experiment setup and the underlying data analysis.

III. EXPERIMENT AND ANALYSIS

The data presented in this work were measured at the 7 MV Van de Graaff accelerator of the IRMM in Geel, Belgium. The neutrons were produced via the reaction D$(d,n)^3$He. A twin Frisch-Grid ionization chamber was used to detect the fission fragments. The chamber was operated with P-10 as counting gas, and the gas pressure was set to 1.05 bar with a gas flow of 0.1 ℓ/min. Further experimental details can be

found in Refs. [19,20]. The two measurements chosen for this study were at incident neutron energies 4 (±0.24) MeV and 5 (±0.17) MeV. Wave-form digitizers were used for data acquisition and digital signal-processing routines for the analysis of the digitized traces from the ionization chamber electrodes [18,19]. Simultaneously, the energy and the emission angle of both fragments were measured. The emission angle was deduced using the grid signal directly as presented in Ref. [20]. To calculate the pre-neutron-emission mass distribution, the double energy method was used. Conservation of mass, kinetic energy, and momentum were employed in an iterative process, where the neutron multiplicity, $\bar{\nu}(A)$, is a crucial parameter. Because the neutron evaporation was not measured and the nuclear data libraries lack neutron data for ^{234}U(n,f), $\bar{\nu}(A)$ was parametrized based on available data from neighboring uranium isotopes ^{233}U and ^{235}U similarly to Ref. [11]. Because the neutron emission from ^{233}U is slightly higher than in ^{235}U according to Fig. 1(a), one may write the ratio as $\bar{\nu}_{235}(A)/\bar{\nu}_{233}(A) = 1 - \beta$, where $\beta \ll 1$. Thus, the ratio $\bar{\nu}_{234}(A)/\bar{\nu}_{233}(A)$ is assumed to be 1–0.5β, owing to the mass difference of one neutron. By combining these relations, one obtains an approximation of the neutron multiplicity as a function of mass for ^{234}U(n,f) as given in Eq. (1):

$$\begin{aligned}\bar{\nu}_{234}(A) &= \bar{\nu}_{233}(A)\left(1 - \frac{1}{2}\beta\right)\\ &= \bar{\nu}_{233}(A)\left[1 - \frac{1}{2}\left(1 - \frac{\bar{\nu}_{235}(A)}{\bar{\nu}_{233}(A)}\right)\right]\\ &= \frac{1}{2}[\bar{\nu}_{235}(A) + \bar{\nu}_{233}(A)]. \qquad (1)\end{aligned}$$

In Fig. 1(a) the resulting neutron multiplicity as a function of fragment mass is shown, based on Eq. (1). It is also compared to the experimental results for ^{233,235}U taken from Ref. [7]. In addition to the mass dependency the neutron emission also depends on the TKE:

$$\nu(A, \mathrm{TKE}) = \bar{\nu}(A) + \frac{\bar{\nu}(A)}{\bar{\nu}(A) + \bar{\nu}(A_{\mathrm{CN}} - A)} \frac{\langle \mathrm{TKE}(A)\rangle - \mathrm{TKE}}{E_{\mathrm{sep}}}, \qquad (2)$$

where $E_{\mathrm{sep}} = 8.6$ MeV is the neutron separation energy, $\langle \mathrm{TKE}(A)\rangle$ is the mean TKE as a function of fragment mass, and TKE is the sum of FF energies for each fission event [10,21]. The full neutron multiplicity distribution after this parametrization is shown in Fig. 2. The neutron multiplicity is taken into account in the iterative calculation to determine the pre-neutron-emission energy,

$$E_{\mathrm{pre}} = \frac{A_{\mathrm{pre}}}{A_{\mathrm{pre}} - \nu(A, \mathrm{TKE})} E_{\mathrm{post}}, \qquad (3)$$

which is finally used to get the pre-neutron-emission masses. From Eq. (2) it is clear that fission events with higher TKE emit less neutrons owing to their lower excitation energy and more compact shape, hence lower deformation energy. The mass and TKE dependencies are the dominating factors in the parametrization of the number of emitted neutrons. However, also the increasing total prompt neutron multiplicity with incident neutron energy, $\bar{\nu}_{\mathrm{tot}}(E_{\mathrm{n}})$, must be accounted for. For this purpose, data from Ref. [8] were chosen. The data points were fitted linearly and used to correct the average neutron multiplicity as a function of mass which entered the iterative calculation [Fig. 1(b)]. The neutron multiplicity shape as calculated from Eq. (1) and shown in Fig. 1(a) is scaled to give a total neutron emission, corresponding to thermal incident neutron energy of ^{234}U(n,f). As stressed earlier, two different neutron-emission correction methods were compared. Based on the AV method, the average increase in neutron multiplicity was shared equally among all fragments. As seen in Fig. 3, this corresponds to an overall higher neutron multiplicity compared to the one calculated from Eq. (1) and shown in Fig. 1(a). In the HE method $\bar{\nu}$ is increased only for heavy fragments. Therefore, the $\bar{\nu}(A)$ distribution remains unchanged for $A < 120$ amu, and $\bar{\nu}(A)$ is increased for $A \geqslant 120$ amu, carefully scaled to conserve the total average neutron multiplicity as given in Fig. 1(b). The choice of $A = 120$ introduces an artificial

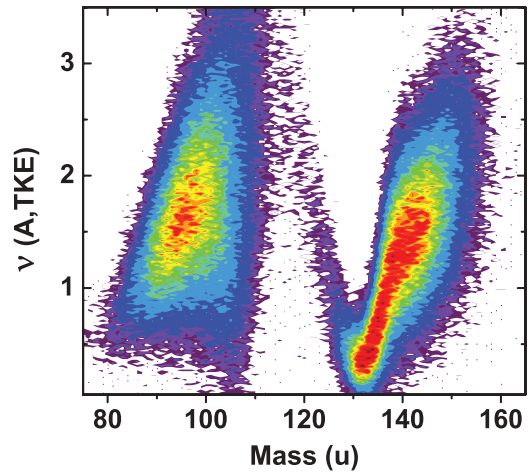

FIG. 2. (Color online) The full neutron multiplicity distribution from Eq. (2) as a function of fragment mass for the (AV) method. The spread of $\nu(A, \mathrm{TKE})$ is attributable to the TKE dependence.

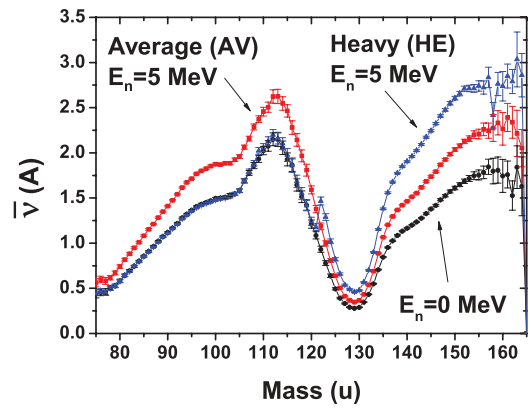

FIG. 3. (Color online) The prompt neutron multiplicity distribution, $\bar{\nu}(A)$, for the three cases discussed in this work: $\bar{\nu}(A)$ taken at thermal incident-neutron energy (black circles), $\bar{\nu}(A)$ distributing the excess neutrons amongst all fission fragments (AV method, red squares), assuming the excess neutrons coming only from the heavy fragments with mass larger than 120 (HE method, blue triangles) increases $\bar{\nu}$ and introduces an artificial step at $A = 120$.

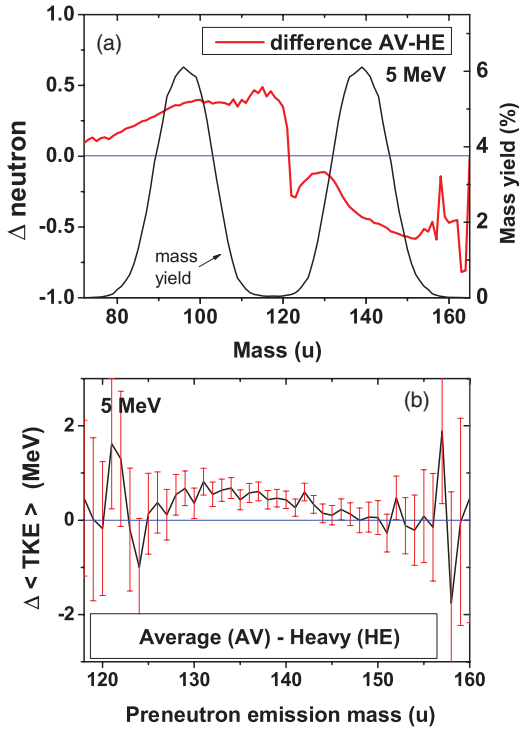

FIG. 4. (Color online) (a) The difference in neutron multiplicity, as a function of mass, between the AV and HE methods. (b) The difference in ⟨TKE (A)⟩ for the AV and HE methods, as a function of fragment mass, A.

increase in $\nu(A)$ visible in Fig. 3. For the sake of clarity, the original neutron multiplicity distribution at thermal neutron energy has also been shown for comparison.

IV. RESULTS AND DISCUSSIONS

A. The dependency of the neutron multiplicity shape on the incident neutron energy

The difference in neutron emission which the two correction methods introduce can be seen in Fig. 4(a) as a function of fragment mass. The average neutron multiplicity for the light and heavy fragments is listed in Table I. We studied the effects of this large difference on the TKE, pre- and post-neutron-emission kinetic energy ($E_{\rm kin}$) and also on the mass distributions (both pre- and postneutron distributions). The average TKE variations are presented in Table II for the $E_{\rm n} = 4$ MeV and $E_{\rm n} = 5$ MeV runs. The AV method showed a higher ⟨TKE⟩, which amounts to 0.2 MeV for the $E_{\rm n} = 5$ MeV case. The difference grows with incident neutron energy. The $\Delta\langle {\rm TKE}(A)\rangle$ is expressed as $\langle {\rm TKE}(A)\rangle_{\rm AV} - \langle {\rm TKE}(A)\rangle_{\rm HE}$. $\Delta\langle {\rm TKE(A)}\rangle$ is slightly mass dependent, as shown in Fig. 4(b), as a function of the pre-neutron-emission mass and it grows for lower mass asymmetry. The case with the noncorrected neutron multiplicity shows a lower TKE. This can be understood considering Eq. (3), because a lower neutron emission, $\nu(A,$ TKE) implies a lower pre-neutron-emission energy $E_{\rm pre}$ relative to the detected energy $E_{\rm post}$. To further explore the impact of the different neutron shapes, we studied the single fragment kinetic energies. The effects found in the post-neutron-emission energies, presented in Fig. 5, were more pronounced compared to the pre-neutron-emission energies. In the heavy-fragment region, the postneutron emission $\langle E_{\rm kin}\rangle$ is up to 0.75 MeV higher, for the AV method. For the light fragments, the $\langle E_{\rm kin}\rangle$ was slightly higher for the HE method. These energy changes were correlated to changes in the mass distributions. Figure 6 shows the mass distribution for the 5 MeV case before and after neutron emission, revealing significant changes in the fragment yield. The post-neutron-emission mass distribution was especially affected, and in terms of $\langle A_{\rm H}\rangle$ twice the shift was encountered (see Table II). The HE method yields a less asymmetric mass distribution, which amounts to a shift of 0.68 amu in the mean heavy FF mass for the $E_{\rm n} = 5$ MeV case. In Fig. 7 the absolute yield difference for each fragment mass is shown. Again, in the post-neutron-emission case, the heavy fragments experience larger deviations. The absolute mass yield is around 0.5% different at fragment masses $A = 90$, 102, 132, and 145, where the largest differences were found between the AV and HE methods. Note that the maximum probable fission yield reaches 6–7%. The relative changes as a function of fragment mass can be seen in Fig. 8, where the ratio between the post-neutron-emission mass distributions (AV/HE) was calculated. The relative changes reach up to 20–30%, for very symmetric or asymmetric mass divisions. The observed changes in mass and TKE distributions were mostly visible on the values of the average distributions and not on the variance of the distribution. At least for the pre-neutron-emission mass distributions, the $\sigma_{\rm TKE}$ and σ_A were within experimental uncertainty, independent of the neutron correction method.

TABLE I. Average prompt neutron multiplicity, $\bar{\nu}$, for the two different methods for neutron emission correction.

Energy (MeV)	No. of events	Neutron-emission correction method	$\bar{\nu}_{\rm light}$	$\bar{\nu}_{\rm heavy}$
4	81 000	No correction	1.355 ± 0.003	1.030 ± 0.003
	81 000	Average (AV)	1.618 ± 0.003	1.243 ± 0.003
	81 000	Heavy (HE)	1.353 ± 0.003	1.516 ± 0.003
5	1 41 000	No correction	1.359 ± 0.002	1.019 ± 0.002
	1 41 000	Average (AV)	1.695 ± 0.002	1.291 ± 0.002
	1 41 000	Heavy (HE)	1.361 ± 0.002	1.633 ± 0.002
5	1 41 000	$\bar{\nu}(^{238}{\rm U})$ (AV)	1.478 ± 0.002	1.503 ± 0.002
5	1 41 000	$\bar{\nu}(^{239}{\rm Pu})$ (AV)	1.533 ± 0.002	1.459 ± 0.002

TABLE II. Characteristic fission-fragment properties for the different methods applied to correct for prompt neutron emission.

Energy (MeV)	Neutron-emission correction method	TKE (MeV)	Preneutron mass $\langle A_H \rangle$	Postneutron mass $\langle A_H \rangle$
4	No correction	169.67 ± 0.04	138.75 ± 0.03	137.76 ± 0.03
	Average (AV)	170.04 ± 0.04	138.83 ± 0.03	137.62 ± 0.03
	Heavy (HE)	169.89 ± 0.04	138.57 ± 0.03	137.09 ± 0.03
5	No correction	169.44 ± 0.03	138.56 ± 0.02	137.59 ± 0.02
	Average (AV)	169.91 ± 0.03	138.66 ± 0.02	137.42 ± 0.02
	Heavy (HE)	169.72 ± 0.03	138.33 ± 0.02	136.74 ± 0.02
5	$\bar{\nu}(^{238}\mathrm{U})$ (AV)	169.79 ± 0.03	138.45 ± 0.02	137.01 ± 0.02
5	$\bar{\nu}(^{239}\mathrm{Pu})$ (AV)	169.82 ± 0.03	138.50 ± 0.02	137.10 ± 0.02

Overall, the choice of the neutron multiplicity shape was found to be very important for the fission characteristics. By applying the HE method, the heavy fragment is assumed to emit more neutrons, while the light fragment emits fewer neutrons compared to the AV method. Thus, the total effect will be that the mass distribution becomes inevitably less asymmetric when applying the HE method and increasing incident neutron energy. This effect was even found to increase for events with smaller TKE, because more neutrons are emitted for those events owing to the larger excitation energy. Furthermore, the differences were found to increase with incident neutron energy, because the $E_n = 5$ MeV case showed larger differences in both TKE and mass compared to $E_n = 4$ MeV. Hence, one may conclude that the choice of neutron emission shape becomes more important for higher incident neutron energies as differences become more visible. Another result from this work is that all observables show a more severe effect in the post-neutron-emission case compared to the pre-neutron-emission one. Hence, if the aim is to analyze the post-neutron-emission masses, increased weight is put on the choice of the shape of the neutron multiplicity.

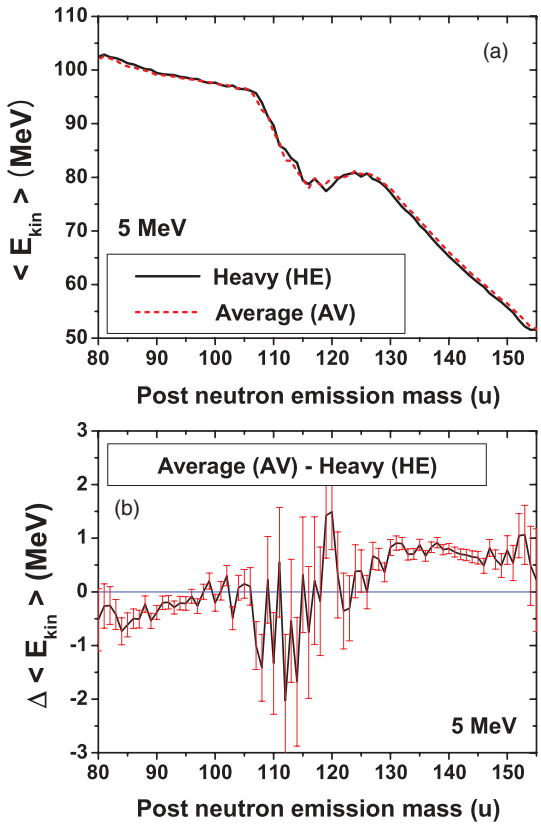

FIG. 5. (Color online) (a) Post-neutron-emission kinetic energy as a function of post-neutron-emission mass for $E_n = 5$ MeV. (b) The difference in $\langle E_{kin} \rangle$ between the AV and the HE methods. A relative change of 0.75 MeV is observed for the heavy fragments.

B. The dependency of the neutron multiplicity on the fragment mass

In the previous section, the different neutron-multiplicity shapes were found to affect the fragment properties. Evidently, if the HE method is applied, the neutron-emission shape changes as a function of the incident neutron energy. These findings stress the importance of the mass dependency of the neutron multiplicity shape. This was discussed briefly in Ref. [11] for $^{238}\mathrm{U}(n,f)$, where different neutron-multiplicity shapes were applied. No significant difference was found on the TKE, if the neutron multiplicity shapes from either $^{238}\mathrm{U}(n,f)$ and $^{239}\mathrm{Pu}(n,f)$ were used. It was found that the most important factor to change the fragment properties was the average $\bar{\nu}$ which needed to be scaled to match the total

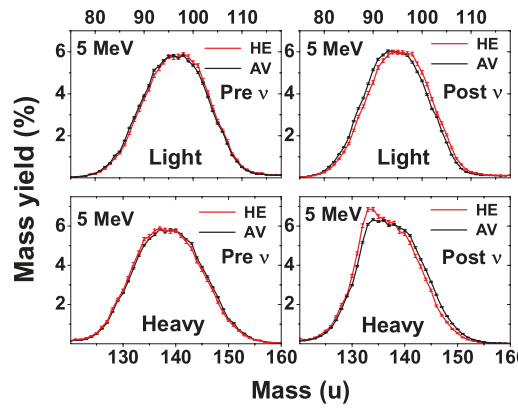

FIG. 6. (Color online) The mass distributions for the 5 MeV case for heavy and light fragments, respectively. The pre-neutron-emission yields are to the left and the post-neutron-emission yields are shown to the right.

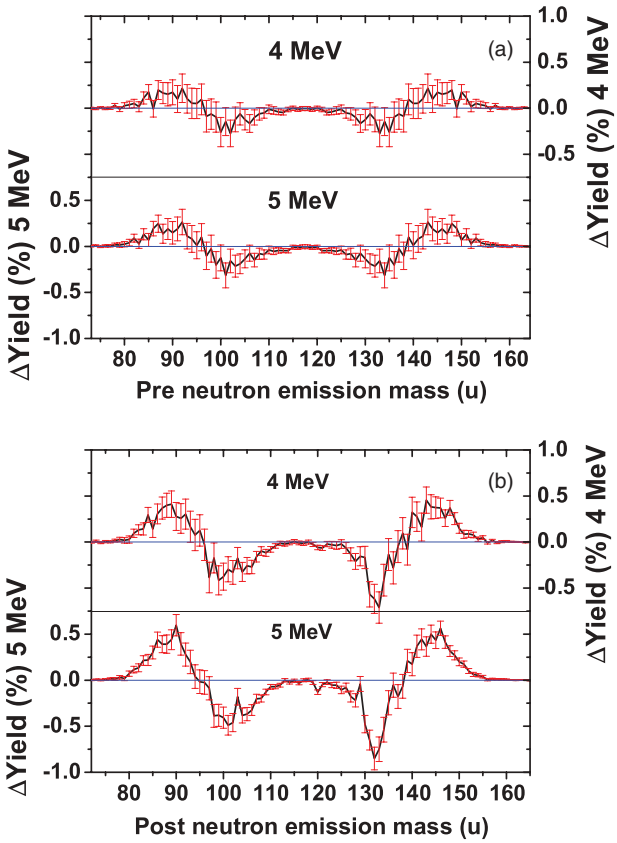

FIG. 7. (Color online) (a) The absolute mass difference of the AV and HE methods, shown for the pre-neutron-emission mass distribution. (b) The corresponding difference in post-neutron-emission mass distribution. Both distributions become more symmetric using the HE method and the differences are larger in the post-neutron-emission case. Note that these are absolute yield differences and that the maximum mass yield is typically 6–7%.

average neutron emission. This conclusion is valid, but only for these relatively similar shapes of the neutron multiplicity as a function of mass. When the shape is considerably different,

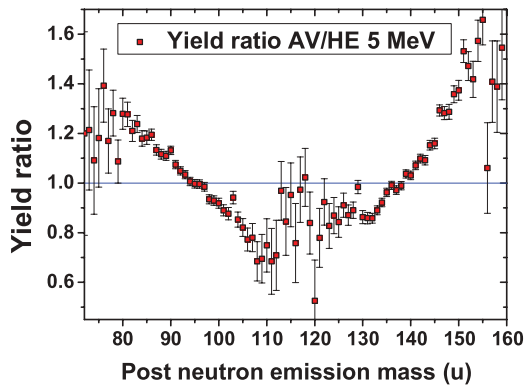

FIG. 8. (Color online) The relative change between the two correction methods, as a function of post-neutron-emission mass. The yield change introduced by the wrong correction method is around 15% for $A = 90$, 102, 132, and 145 and may reach 20–30% for very symmetric or asymmetric masses.

such as in the case of the HE vs AV methods, this cannot be true anymore and the shape itself plays a great role. The neutron multiplicity distributions used in Ref. [11] for ^{238}U and ^{239}Pu show a similar shape [see Fig. 1(a)]. So after scaling them to the incident neutron energy, the neutron emission will be almost the same regardless of which distribution was used. To test these arguments, we also applied the neutron multiplicity shapes from ^{238}U and ^{239}Pu to the 5 MeV case. The two normalized shapes yielded almost equal neutron emission from each of the light and heavy fragments as seen in Table I. Because the shapes are so similar, the observed changes in TKE and mean mass were small (Table II), which confirms the results of Ref. [11]. However, when the shape undergoes major changes, such as is the case with the AV vs HE methods, considerable differences emerge. The average change of the neutron multiplicity from each of the heavy and light fragments, provides a measure of the estimated effect. The difference in average neutron multiplicity per fragment is below 4% between the shapes of ^{238}U and ^{239}Pu. However, when comparing the AV and HE methods, the neutron multiplicity is, on average, different by 26% per fragment. Finally, we estimated the potential errors in TKE and mean heavy mass, introduced by a wrong total average neutron emission. As seen in Fig. 9(a), for each extra neutron in the total neutron emission, the TKE and mean heavy mass increased by roughly 0.76 MeV and 0.16 amu. The total average neutron emission is thus crucial to correct for, because it otherwise leads to considerable changes in the fission observables.

C. Conversion between the methods

Numerous fission measurements performed with the double-E technique were analyzed based on the AV method. It could be of use to provide an estimation of the conversion factor for the two correction methods. As stressed earlier, up to this date, we cannot conclusively favor either of the correction methods. However, we can estimate the change expected from applying the HE method instead of the AV method. In Eqs. (4) and (5), two relations are given to convert the TKE and the pre-neutron-emission mean fragment mass. Because σ_{TKE} and σ_A are practically unchanged when applying either correction method, these relations can provide a good approximation to the expected shift in $\langle A^{\mathrm{pre}}\rangle$ and $\langle \mathrm{TKE}\rangle$. These relations serve primarily for $^{234}\mathrm{U}(n,f)$, where a similar neutron emission shape was used, as the parametrized one from Fig. 1(a). In case of other fissioning system studies, the relations could also be applied, but would indicate only a rough estimation of the change in TKE and mean mass. The following relations were obtained by fitting the change in terms of $\langle \mathrm{TKE}\rangle$ and mean mass as a function of the incident neutron energy, E_{n}, as seen in Fig. 9(b) and 9(c). The changes fitted were $\Delta\langle \mathrm{TKE}\rangle = \langle \mathrm{TKE}\rangle_{\mathrm{AV}} - \langle \mathrm{TKE}\rangle_{\mathrm{HE}}$ and $\Delta\langle A_{\mathrm{H}}\rangle = \langle A_{\mathrm{H}}\rangle_{\mathrm{AV}} - \langle A_{\mathrm{H}}\rangle_{\mathrm{HE}}$. The fits were directly proportional to the incident neutron energy, thus providing a linear conversion relation for both observables:

$$\langle \mathrm{TKE}\rangle_{\mathrm{HE}} \approx \langle \mathrm{TKE}\rangle_{\mathrm{AV}} - 0.038 \times E_{\mathrm{n}} \ \ (\mathrm{MeV}), \qquad (4)$$

$$\left\langle A_{\mathrm{H}}^{\mathrm{pre}}\right\rangle_{\mathrm{HE}} \approx \left\langle A_{\mathrm{H}}^{\mathrm{pre}}\right\rangle_{\mathrm{AV}} - 0.065 \times E_{\mathrm{n}} \ \ (\mathrm{amu}). \qquad (5)$$

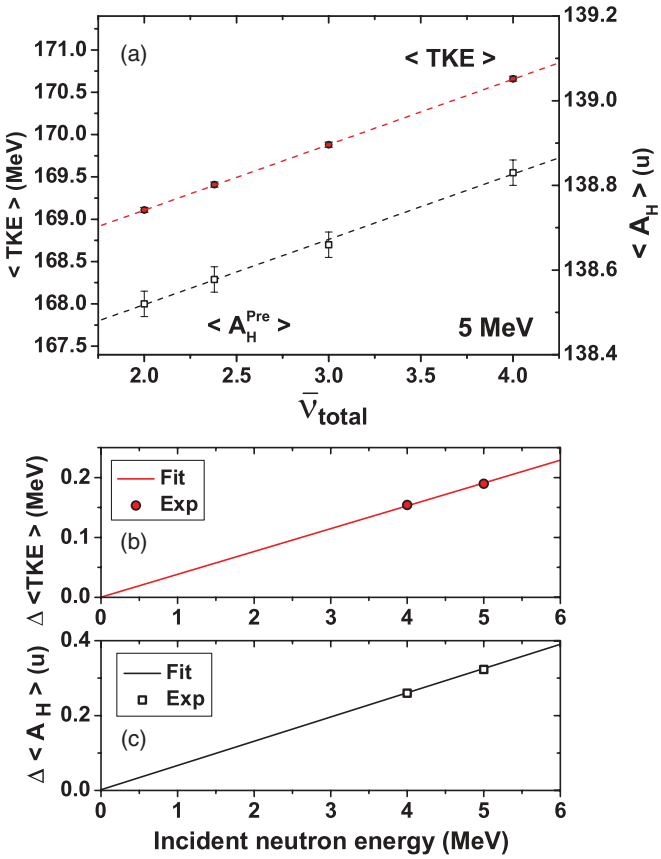

FIG. 9. (Color online) (a) The TKE and mean pre-neutron-emission mass as a function of the total neutron emission for the AV method. The original parametrization from Eq. (1) was scaled to the different $\bar{\nu}$ values. The change in $\langle \mathrm{TKE} \rangle$ (b) and pre-neutron-emission mass, $\langle A_{\mathrm{H}} \rangle$ (c), for the two approaches, fitted linearly.

Finally, the conversion for the post-neutron-emission masses is given in Eq. (6). However, as found in this work, these post-neutron-emission distributions showed severe changes also in the details of the energy and mass distributions. A mere average shift of the distribution is probably not sufficient to assess the real effect of the two correction methods:

$$\left\langle A_{\mathrm{H}}^{\mathrm{post}} \right\rangle_{\mathrm{HE}} \approx \left\langle A_{\mathrm{H}}^{\mathrm{post}} \right\rangle_{\mathrm{AV}} - 0.135 \times E_{\mathrm{n}} \ \ (\mathrm{amu}). \tag{6}$$

V. CONCLUSIONS

In this study we have investigated two different methods of correction for the prompt neutron emission in neutron-induced fission as a function of fragment mass using the reaction $^{234}\mathrm{U}(n,f)$ at 4 and 5 MeV incident neutron energies as example. The increased neutron multiplicity for higher incident neutron energies is either distributed among all fission fragments, labeled as the AV method, or shared only by the heavy fragments, labeled as the HE method. The distribution, $\bar{\nu}(A)$ was always normalized properly to obtain the total average neutron multiplicity, $\bar{\nu}_{\mathrm{tot}}$, measured at the corresponding incident neutron energy E_{n} [8]. The following list summarizes the outcome of this work.

(i) First we consider the shape of $\bar{\nu}(A)$. The shape of the neutron emission as a function of fragment mass was found to affect the fission observables dependent on how different the shape of the $\bar{\nu}(A)$ distribution is. By using the relatively similar shapes of $^{239}\mathrm{U}^*$ and $^{240}\mathrm{Pu}^*$, no big difference was found. However, when using relatively different $\bar{\nu}(A)$ shapes, for example, as used in the AV vs HE method, much larger effects are observed, and the choice of the distinct shape of the $\bar{\nu}(A)$ distribution becomes crucial. A lower TKE was observed using the HE method, which amounts to a decrease of 0.2 MeV in the most severe case. The HE method resulted in a lower kinetic energy for the heavy fragments in the post-neutron-emission case. In addition, the relative yield change in post-neutron-emission mass yield was about 15% for yields around $A = 90$, 102, 132, and 145 amu. For very symmetric or asymmetric mass divisions, the relative changes reached up to 30%.

(ii) Using the HE method the mass distribution becomes more symmetric. The average post-neutron-emission mass shifted by 0.68 amu in the most severe case. The effect is double for the post-neutron-emission masses compared to the pre-neutron-emission mass distributions. Thus, the choice of method becomes more critical, when information about the post-neutron-emission masses are essential.

(iii) As the observed changes in the fragment distributions depend on incident neutron energy, the choice of either neutron multiplicity distribution would play a greater role for measurements at higher incident neutron energies. A numerical estimation is proposed in Eqs. (4)–(6) to serve for a conversion between the characteristic fragment properties obtained with the two methods. It was estimated that the difference in the two methods are $0.038 \times E_{\mathrm{n}}$ MeV for the TKE, $0.065 \times E_{\mathrm{n}}$ amu for the pre-neutron-emission mass distribution, and $0.135 \times E_{\mathrm{n}}$ amu for the post-neutron-emission mass distribution.

Finally, we would like to point out that, although experimental data favor the HE method for prompt neutron correction, our analysis may not be taken as validation or disproof for any of these two methods. However, because the reliable assessment of fission fragment properties, in particular those after prompt neutron emission, is essential for the inventory of nuclear waste as well as for the delayed-neutron precursor yields, efforts should be made in the near future to measure prompt neutron emission at nonthermal neutron energies in full correlation with fission fragments. Those data would be of great help to further improve our knowledge about the share of excitation energy between fission fragments.

ACKNOWLEDGMENTS

The authors would like to thank the staff of the Van de Graaff accelerator at the IRMM Geel, Belgium, for providing a stable neutron beam. One of us (A.A.) would like to thank EC-JRC-IRMM for financial support, via a grant from the European Commission.

[1] R. Vandenbosch and J. R. Huizenga, *Nuclear Fission* (Academic Press, San Diego, 1973).
[2] A. A. Naqvi, F. Käppeler, F. Dickmann, and R. Müller, Phys. Rev. C **34**, 218 (1986).
[3] R. Müller, A. A. Naqvi, F. Käppeler, and F. Dickmann, Phys. Rev. C **29**, 885 (1984).
[4] K.-H. Schmidt and B. Jurado, Phys. Rev. Lett. **104**, 212501 (2010).
[5] K.-H. Schmidt and B. Jurado, Phys. Rev. C **83**, 061601 (2011).
[6] C. Manailescu, A. Tudora, F.-J. Hambsch, C. Morariu, and S. Oberstedt, Nucl. Phys. A **867**, 12 (2011).
[7] A. C. Wahl, At. Data Nucl. Data Tables **39**, 1 (1988).
[8] D. S. Mather, P. Fieldhouse, and A. Moat, Nucl. Phys. **66**, 149 (1965).
[9] J. Teller, Phys. Rev. **127**, 880 (1962).
[10] E. Birgersson, A. Oberstedt, S. Oberstedt, and F.-J. Hambsch, Nucl. Phys. A **817**, 1 (2009).
[11] F. Vivés, F.-J. Hambsch, H. Bax, and S. Oberstedt, Nucl. Phys. A **662**, 63 (2000).
[12] J. P. Lestone, Nucl. Data Sheets **112**, 3120 (2011).
[13] R. Vogt, J. Randrup, D. A. Brown, M. A. Descalle, and W. E. Ormand, Phys. Rev. C **85**, 024608 (2012).
[14] C. J. Bishop, R. Vandenbosch, R. Aley, R. W. Shaw, and I. Halpern, Nucl. Phys. A **150**, 129 (1970).
[15] S. C. Burnett, R. L. Ferguson, F. Plasil, and H. W. Schmitt, Phys. Rev. C **3**, 2034 (1971).
[16] M. Strecker, R. Wien, P. Plischke, and W. Scobel, Phys. Rev. C **41**, 2172 (1990).
[17] T. von Egidy and D. Bucurescu, Phys. Rev. C **72**, 044311 (2005).
[18] A. Al-Adili, F.-J. Hambsch, S. Oberstedt, and S. Pomp, Phys. Procedia **31**, 158 (2012).
[19] A. Al-Adili, F.-J. Hambsch, S. Oberstedt, S. Pomp, and S. Zeynalov, Nucl. Instrum. Methods Phys. Res., Sect. A **624**, 684 (2010).
[20] A. Al-Adili, F.-J. Hambsch, R. Bencardino, S. Pomp, S. Oberstedt, and S. Zeynalov, Nucl. Instrum. Methods Phys. Res., Sect. A **671**, 103 (2012).
[21] G. Barreau, A. Sicre, F. Caïtucoli, M. Asghar, T. P. Doan, B. Leroux, G. Martinez, and T. Benfoughal, Nucl. Phys. A **432**, 411 (1985).